Maximum Torque Control of 3-phase induction motor drives

PIOTR WACH

Politechnika Opolska
e-mail: p.wach@po.opole.pl

Abstract: Maximum Torque Control (MTC) is a new method applied for control of induction motor drives. The drive is controlled by dc voltage supplying a converter in the range below nominal speed and by a field that weakens for a speed range above the nominal speed. As a consequence, the control is quite similar to the control of a classical separately excited dc motor. This control method could be explained as a kind of simplification of Direct Torque Control (DTC), because the switching scheme is the same as for the DTC, but the variable responsible for a torque control is constantly set for "torque increase". This kind of control of induction motor drive is simpler than DTC because torque values need not be estimated. The proposed control method offers very good performance for 3-phase induction motors and requires smaller switching frequency in comparison to DTC and Field Oriented Control (FOC). The application of the control is widely demonstrated for a 3-phase 315 kW, 6 kV motor drive by use of computer simulation.

Key words: induction motor control, angular velocity control, direct torque control, field oriented control, DC-AC power converters, Maximum Torque Control

1. Introduction

The control of 3-phase induction motors by use of dc/ac converters seems to be well explored and was described in many papers [1, 5, 2] and books [6, 7]. There is a variety of advanced methods of control of such drives [4, 12, 15, 16] but they mainly fall into two categories: Field Oriented Control (FOC) and Direct Torque Control (DTC). Both these methods require similar computation effort and yield comparable results [1, 3, 5, 11]. This result does not come as a surprise since a 3-phase single level converter offers 8 switching states only. But still the combination of switching states, their duration and frequency offer a potential to implement a novel control. In this paper a new method called Maximum Torque Control (MTC) is presented and explained in relation to DTC and FOC. The adjective "maximum" could be eas-

ily explained comparing this method to DTC. If we take the switching table for DTC we find two variables, whose combination determines the choice of next switching state – one that is responsible for a change of the magnetic field and the second one responsible for a change of electromagnetic torque. In the case of the proposed new MTC method the variable for torque control is set "torque up" constantly. As a result, the switching table is reduced to two rows only – one for "field increase" and the other one for "field decrease". The practical effect of such control is that torque always follows its accessible extremes, and control of the rotational speed is performed by dc voltage value supplying the converter for a speed range below the rated value, and by a field weakening for speed above the nominal. These work very well and are closely similar to the old traditional methods of control of separately excited dc motors with a commutator. The term "Maximum Torque Control" is present in the literature but has taken on a different meaning. In [10] it is a problem of a maximum torque per ampere in the field weakening region of control, in [14] a problem of finding an optimal frequency of supply voltage, and in [13] it is a control of permanent magnet synchronous motors. Hence, the Maximum Torque Control (MTC) proposed here offers an original control method, derived from DTC, but resulting in control of an induction machine quite similar to the control of separately excited dc motors and yielding similar characteristics. The following sections of the paper will explain the theoretical basis for MTC control and its relations to DTC and FOC, and will present wide illustration of its application to the 315 kW, 6 kV 3-phase induction motor – resulting from computer simulations.

2. Mathematical models

To explain MTC and its relationship to FOC and DTC, it is necessary to present the mathematical models of induction machines in orthogonal axes using (Ψ_s, i_s) and (Ψ_r, i_s) variables. For (Ψ_s, i_s), the model takes the form, as in [8]:

$$\dot{\Psi}_{sx} = u_{sx} - R_s i_{sx} + \Omega_0 \Psi_{sy},$$

$$\dot{\Psi}_{sy} = u_{sy} - R_s i_{sy} - \Omega_0 \Psi_{sx},$$

$$\dot{i}_{sx} = (\alpha_r \Psi_{sx} + p\Omega_r \Psi_{sy} + u_{sx})/(L_s\sigma) - (\alpha_s + \alpha_r)i_{sx}/\sigma + p\Omega_0 s i_{sy},$$

$$\dot{i}_{sy} = (\alpha_r \Psi_{sy} - p\Omega_r \Psi_{sx} + u_{sy})/(L_s\sigma) - (\alpha_s + \alpha_r)i_{sy}/\sigma - p\Omega_0 s i_{sx},$$ (1)

$$\dot{\Omega}_r = [\underbrace{p(\Psi_{sx}i_{sy} - \Psi_{sy}i_{sx})}_{T_e} - T_l - D\Omega_r]/J,$$

where: Ψ_{sx}, Ψ_{sy} are stator flux transformed to x, y axes, i_{sx}, i_{sy} are stator currents transformed to x, y axes, u_{sx}, u_{sy} are stator voltages transformed to x, y axes, L_s, L_r, L_m are stator, rotor and magnetizing inductances, R_s, R_r are stator, rotor, windings' resistances, $\alpha_s = R_s/L_s$ is a stator winding's damping coefficient, $\alpha_r = R_r/L_r$ is a rotor winding's damping coefficient, $\sigma = 1 - k_s k_r$ is a winding's leakage factor, $k_s = L_m/L_s$ is a stator winding's coupling coefficient, $k_r = L_m/L_r$ is a rotor winding's coupling coefficient, $\Omega_0 = 2\pi f_s/p$ is angular speed of a magnetic field, Ω_r is an angular speed of a rotor, $s = (\Omega_0 - \Omega_r)/\Omega_0$ is a slip of a rotor, T_e, T_l are electromagnetic

torque and load torque respectively. Equations (2) constitute a mathematical model of induction motor drive for (Ψ_r, i_s):

$$\dot{\Psi}_{rx} = -\alpha_r(\Psi_{rx} - L_m i_{sx}) + p\Omega_0 s \Psi_{ry},$$

$$\dot{\Psi}_{ry} = -\alpha_r(\Psi_{ry} - L_m i_{sy}) - p\Omega_0 s \Psi_{rx},$$

$$\dot{i}_{sx} = (k_r \alpha_r \Psi_{sx} + k_r p \Omega_r \Psi_{sy} + u_{sx})/(L_s \sigma) - \gamma i_{sx} + p\Omega_0 s i_{sy},$$

$$\dot{i}_{sy} = (k_r \alpha_r \Psi_{sy} - k_r p \Omega_r \Psi_{sx} + u_{sy})/(L_s \sigma) - \gamma i_{sy} - p\Omega_0 s i_{sx},$$

$$\dot{\Omega}_r = [\underbrace{pk_r(\Psi_{rx} i_{sy} - \Psi_{ry} i_{sx})}_{T_e} - T_l - D\Omega_r]/J,$$

$$(2)$$

where $\gamma = (\alpha_s + \alpha_r k_s k_r)/\sigma$.

By transforming variables in (1) in the following way:

$$(\Psi_{sx}, \Psi_{sy}, i_{sx}, i_{sy}, \Omega_r) \rightarrow (\tau, \Psi_s, i_{x\tau}, i_{y\tau}, \Omega_r),$$

we obtain the model of an induction motor transformed to orthogonal x_τ, y_τ axes. These axes are oriented in respect to x, y axes by use of the angle τ so that the x_τ axis coincides with the direction of Ψ_s vector (Fig. 1). The transformed model (3) is particularly useful for DTC.

$$p\dot{\tau} = (u_{y\tau} - R_s i_{y\tau})/\Psi_s - p\Omega_0,$$

$$\dot{\Psi}_s = u_{x\tau} - R_s i_{x\tau},$$

$$\begin{bmatrix} \dot{i}_{x\tau} \\ \dot{i}_{y\tau} \end{bmatrix} = \frac{1}{L_s \sigma} \begin{bmatrix} u_{x\tau} + \alpha_r \Psi_s \\ u_{y\tau} - p\Omega_r \Psi_s \end{bmatrix} + \begin{bmatrix} -(\alpha_s + \alpha_r/\sigma) & p(\dot{\tau} + \Omega_0 s) \\ -p(\dot{\tau} + \Omega_0 s) & -(\alpha_s + \alpha_r)/\sigma \end{bmatrix} \begin{bmatrix} i_{x\tau} \\ i_{y\tau} \end{bmatrix}, \quad (3)$$

$$\dot{\Omega}_r = [\underbrace{p\Psi_s i_{y\tau}}_{T_e} - T_l - D\Omega_r]/J.$$

A similar transformation of the mathematical model (2) is made $(\Psi_{rx}, \Psi_{ry}, i_{sx}, i_{sy}, \Omega_r) \rightarrow (\rho, \Psi_r, i_{x\rho}, i_{y\rho}, \Omega_r)$, introducing ρ angle as the new variable orienting x_ρ, y_ρ coordinate system
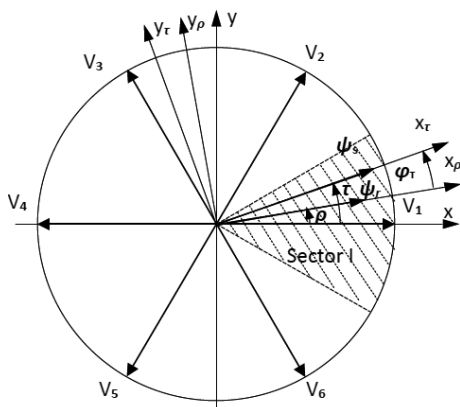
Fig. 1. Orthogonal reference frames for transformed induction motor models, and voltage vectors

in respect to x, y axes of the original system, where the rotor flux vector Ψ_r determines the direction of x_ρ. Consequently, we receive:

$$p\dot\rho = L_m\alpha_r i_{y\rho}/\Psi_r - p\Omega_0 s,$$

$$\Psi_r = -\alpha_r\Psi_r + L_m\alpha_r i_{x\rho},$$

$$\begin{bmatrix} i_{x\rho} \\ i_{y\rho} \end{bmatrix} = \frac{1}{L_s\sigma}\begin{bmatrix} u_{x\rho} + k_r\alpha_r\Psi_r \\ u_{y\rho} - p\Omega_r\Psi_r \end{bmatrix} + \begin{bmatrix} -\gamma & p(\dot\rho + \Omega_0 s) \\ -p(\dot\rho + \Omega_0 s) & -\gamma \end{bmatrix}\begin{bmatrix} i_{x\rho} \\ i_{y\rho} \end{bmatrix}, \qquad (4)$$

$$\dot\Omega_r = [\underbrace{pk_r\Psi_r i_{y\rho}}_{T_e} - T_l - D\Omega_r]/J.$$

The mathematical models in (3), (4) are applicable in the design of DTC and FOC and provide valuable information regarding the steady state of the drive. From (3), for $\dot\tau = 0$, we find the angular speed of the magnetic field:

$$p\Omega_0 = (u_{y\tau} - R_s i_{y\tau})/\Psi_s \qquad (5)$$

and for $\dot\Psi_s = 0$, magnetizing current:

$$i_{x\tau} = u_{x\tau}/R_s. \qquad (6)$$

From (4), for a steady state, we can determine the angular speed of slip $p\Omega_0 s = L_m\alpha_r i_{y\rho}/\Psi_r = R_r T_e/(p\Psi_r^2)$. It is proportional to the rotor's resistance and the torque, and inversely proportional to the square of the rotor flux. In addition, we can learn that $\Psi_r = L_m i_{x\rho}$. At the end of these considerations it is necessary to say that the two above presented mathematical models are not precise or more clearly rigorous. The equation system presented in x, y perpendicular axes, that is applied here is developed [8] with the assumption, that the reference x, y axes rotate with a constant angular velocity Ω_0, which is never the case when frequency f_s changes, and in addition angle ρ may also not be a constant value. On the margin we have to note, that the same remark applies to equations transformed to the d, q axes, which rotate with a speed of the rotor Ω_r, in the case that the speed is not constant. In fact, the most general is an α, β two-axes equation system, in which the reference axes are immobile in respect to the stator, but in that case, we would not be able to develop an effective and easy to interpret control.

3. Explaining Maximum Torque Control method

As we can see from Fig. 2, the angular distance between coordinate systems τ and ρ is small (5° to 10°) and is called "torque angle". An expression of this is given by the following formula for electromagnetic torque:

$$T_e = pk_r\Psi_s\Psi_r\sin(\phi_T),$$

where $\phi_T = \tau - \rho$ is the torque angle. The dynamics of the torque angle is:

$$p\dot\phi_T = p(\dot\tau - \dot\rho) = (u_{y\tau} - R_s i_{y\tau})/\Psi_s - L_m\alpha_r i_{y\tau}/\Psi_r - p\Omega_r. \qquad (7)$$
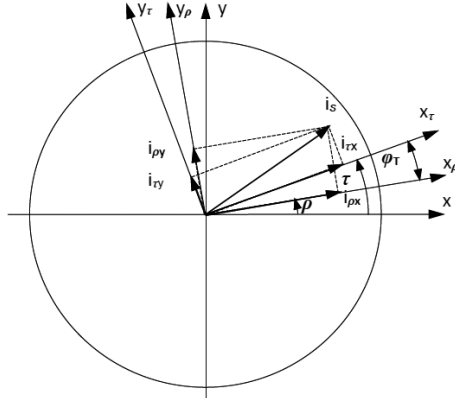
Fig. 2. Explaining the torque angle φ_T

Rough estimations of (7) lead to the following assumptions $i_{y\tau} = i_{y\rho} = i_y$ and $\Psi_s = \Psi_r = \Psi$. By adopting these assumptions, the equation in (7) takes the form:

$$p\dot{\phi}_T = [u_{y\tau} - (R_s + k_r R_r)i_y]/\Psi - p\Omega_r. \tag{8}$$

From (8), we can see that an increase of $u_{y\tau}$ voltage is followed by an adequate increase in the torque T_e. Consequently, a new balance is established resulting from transient courses of i_y current and angular speed Ω_r. Thus, MTC involves the selection of a converter state which ensures the highest value of $u_{y\tau}$. In fact, this choice is limited to two output vectors of the converter being the closest, in angular distance, to a line perpendicular to the axis of a sector in which Ψ_s lies (Fig. 3). For example, under an assumption that that Ψ_s vector is in sector I, we use either of V_2 or V_3 output vectors of the converter to control the drive. V_2 vector is applied for the case when Ψ_s magnetic field vector has to increase, whereas V_3 when the magnetic field should decrease. Table 1 contains MTC switching states for all six sectors of the control plane and this table is much simpler than the one for DTC, because it contains two rows only – one for the field increase (FU) and the other one for the field decrease (FD).

Table 1. MTC control vectors for 3-phase induction motor

Sector	I	II	III	IV	V	VI
FU	V_2	V_3	V_4	V_5	V_6	V_1
FD	V_3	V_4	V_5	V_6	V_1	V_2

Such a selection of the switching states offers a clear advantage of relatively low switching frequency, but its disadvantage is associated with the rather high $u_{y\tau}$ voltage fluctuation $u_{y\tau} = cU_{dc}\cos(\phi_s - 30°)$, where ϕ_s is the angle measured from the axis of a sector in which Ψ_s vector lies. The range of ϕ_s is $\phi_s = \langle -30°, 30° \rangle$ and hence,

$$u_{y\tau}/U_{dc} = c \langle 0.5, 1.0 \rangle . \tag{9}$$
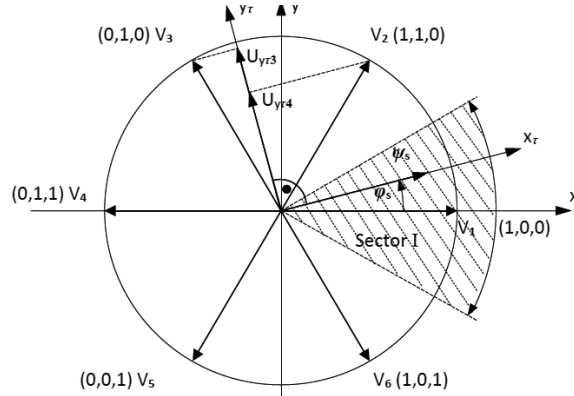
Fig. 3. Switching states for 3-phase converter supplying induction motor

A constant c in (9) depends slightly on $u_{x\tau} = R_s i_{x\tau}$ and is close to the 0.67 value. The pulsations of stator currents and the torque resulting from such voltage fluctuations are much limited, as it is demonstrated later in this work.

4. Transient and steady state characteristics

From (3) we can see that the interaction between the transformed stator currents $i_{x\tau}$ and $i_{y\tau}$, by $(\dot{\tau} + \Omega_0 s)$ factor, is a weak one. This interaction is even more negligible for a small slip values. As a result of adopting the assumption that $(\dot{\tau} + \Omega_0 s) = 0$, it is possible to find a transfer function $U_{dc}(\widetilde{s}) \rightarrow \Omega_r(\widetilde{s})$ and study the transient characteristic of the drive. The other necessary assumption is a constant proportion of $u_{y\tau}/U_{dc}$, which according to (9), is a simplification. The transformed operator equations, respecting a constant value of the stator flux Ψ_s take the form:

$$
\begin{bmatrix}
J\widetilde{s} + D & -p\Psi_s \\
\dfrac{p\Psi_s}{L_s\sigma} & \widetilde{s} + \dfrac{\alpha_s + \alpha_r}{\sigma}
\end{bmatrix}
\begin{bmatrix}
\Omega_r(\widetilde{s}) \\
i_{y\tau}(\widetilde{s})
\end{bmatrix}
=
\begin{bmatrix}
-T_l \\
\dfrac{u_{y\tau}}{L_s\sigma}
\end{bmatrix}.
\tag{10}
$$

With the minor assumption, $D = 0$, Equations (10) lead to the transfer function for the speed of the drive.

$$
\Omega_r(\widetilde{s}) = \frac{-\left(\widetilde{s} + \dfrac{\alpha_s + \alpha_r}{\sigma}\right) T_l + \dfrac{p\Psi_s}{L_s\sigma} u_{y\tau}}{J\left(\widetilde{s}^2 + \dfrac{\alpha_s + \alpha_r}{\sigma}\widetilde{s} + \dfrac{p^2\Psi_s^2}{JL_s\sigma}\right)},
\tag{11}
$$

where $\widetilde{s}$ is the Laplace transform operator. The discriminant of the denominator of (11) is:

$$
\Delta = \left(\frac{\alpha_s + \alpha_r}{\sigma}\right)^2 - \frac{4p^2\Psi_s^2}{JL_s\sigma}.
\tag{12}
$$

The oscillatory character of the transient courses is for $\dfrac{4p^2\Psi_s^2}{JL_s\sigma} > \dfrac{\alpha_s + \alpha_r}{2\sigma}$, the damping factor is $\exp\left(-\dfrac{\alpha_s + \alpha_r}{2\sigma}\right)$, while the pulsation of oscillations equals to

$$\Omega_{\mathrm{osc}} = \sqrt{\frac{p^2\Psi_s^2}{JL_s\sigma} - \left(\frac{\alpha_s + \alpha_r}{2\sigma}\right)^2}.$$

Equations (10)–(12) are strictly similar to the respective equations for transients of separately excited dc motors, if only we substitute the parameters

$$\frac{\alpha_s + \alpha_r}{\sigma} \to \alpha_t = \frac{R_t}{L_t}, \qquad \Psi_s \to \Psi_e, \qquad L_s\sigma \to L_t, \tag{13}$$

where: R_t is an armature resistance of dc motor, L_t is an armature inductance and Ψ_e is an excitation flux.

Mathematical model (3) makes it possible to calculate the steady state characteristics of an induction motor controlled by MTC. A set of figures show some steady state curves, just to illustrate combined features of separately excited dc and induction motor characteristics of this kind of drive.
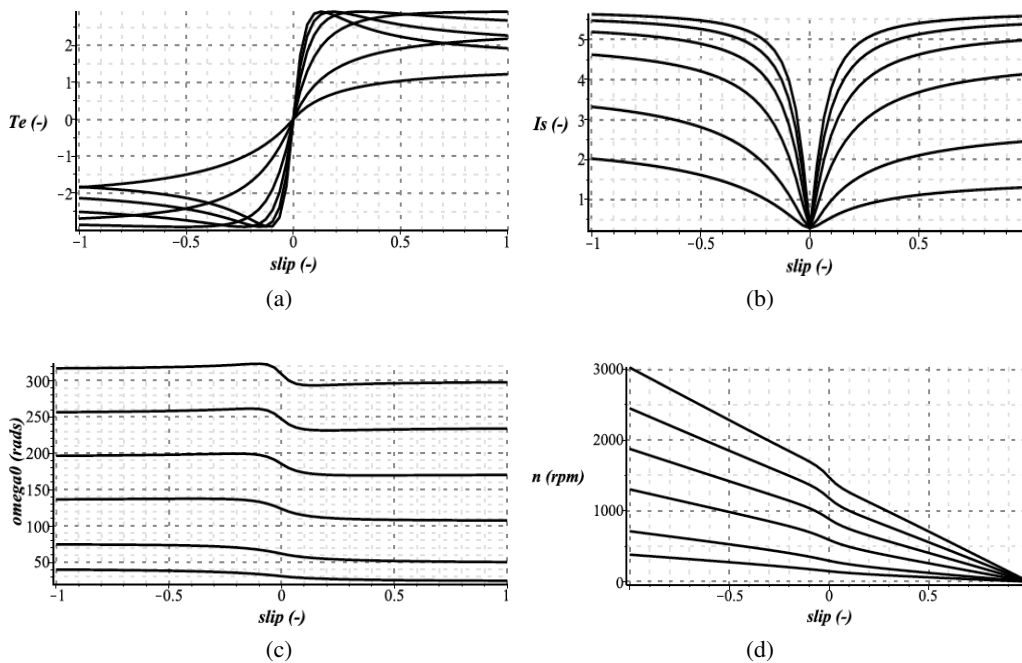
Fig. 4. Steady-state curves for the 315 kW, 6 kV induction motor drive: (a) torque; (b) stator current; (c) rotating field speed; (d) rotor speed, versus slip, for $U_{dc} = (1.0, 0.8, 0.6, 0.4, 0.2, 0.1)U_{dcn}$
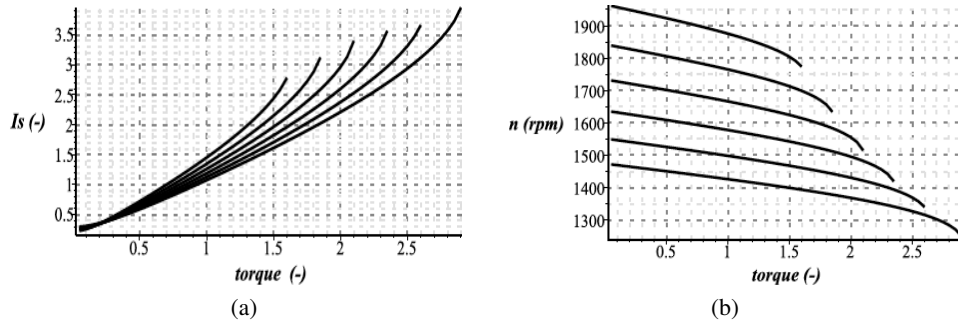
Fig. 5. Steady-state curves for the 315 kW, 6 kV induction motor drive: (a) stator current; (b) speed of
the rotor, versus torque, for stator magnetic field $\Psi_s = (1.0, 0.95, 0.9, \ldots, 0.75)\Psi_n$
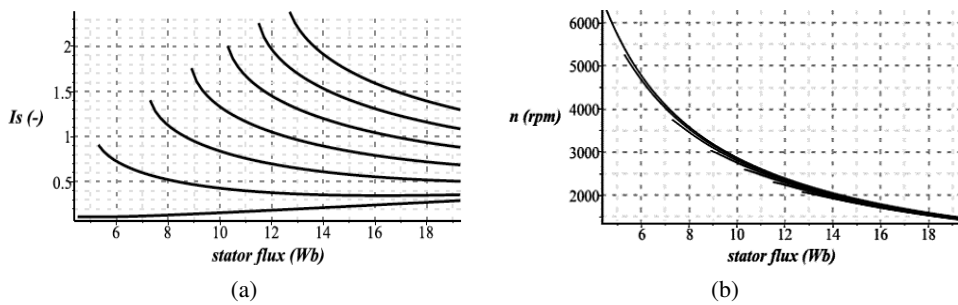
Fig. 6. Steady-state curves for the 315 kW, 6 kV induction motor drive: (a) stator current; (b) rotor
speed, versus stator flux, for different load torque values $T_l = (1.2, 1.0, 0.8, 0.6, 0.4, 0.2, 0.0)T_n$
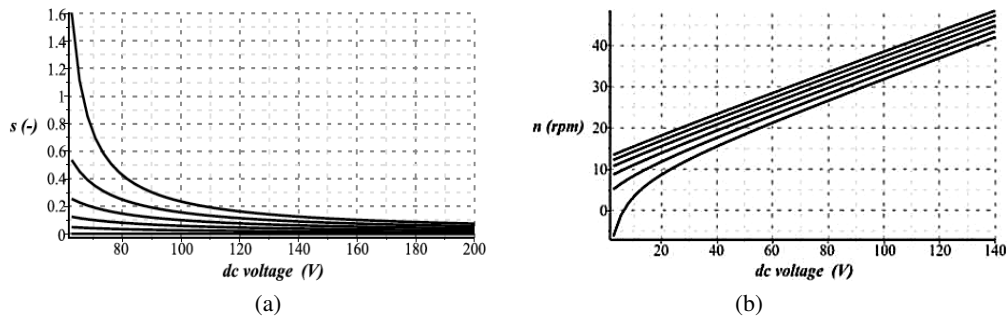
Fig. 7. Steady-state curves for the 315 kW, 6 kV induction motor drive: (a) slip of the rotor; (b) rotor
speed as a function of dc supply voltage U_{dc} (in the range of low voltages), for different load $T_l =$
$(0.1, 0.075, 0.05, 0.025, 0)T_n$

5. MTC dynamics simulations for 3-phase induction motor drives

We can remark at this point that all mathematical models [8, 9] used in simulations of dy-
namics have untransformed stator winding circuits with a star connection point, and the switches
directly operate within the controlled circuits. At first, we present free acceleration course for

a 3-phase induction motor with following rated parameters: $U_n = 6$ kV, $P_n = 315$ kW, $p = 2$, $T_n = 2030$ Nm, and $\Psi_s = 19.5$ Wb controlled within $\pm 6\%$ band. The supply voltage to the converter is $U_{dc} = 8\,600$ V.

An important characteristic of this control is associated with the sampling period, understood as the period between the consecutive control decisions concerning the change of the converter's state by switching or continuation of a current state. In the courses presented in Fig. 8–11, the value of the dead time is 200 μs, which gives a maximum switching frequency of 5 kHz, whereas the actual switching frequency is 3.2 kHz. The course of the frequency f_s (Fig. 8d) could be explained on the basis of analysis of the first equation in (3) and (4). The high frequency at the

(a)

(b)

(c)

(d)

(e)

(f)
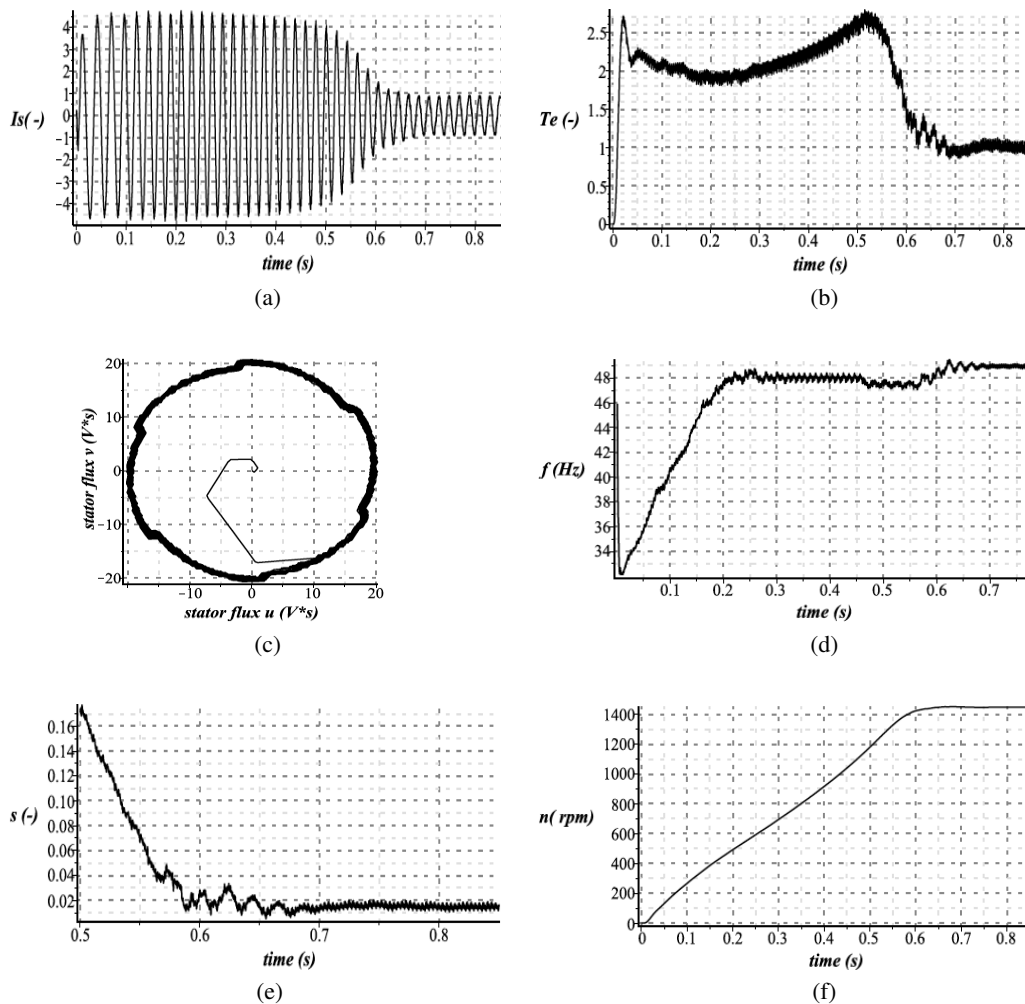
Fig. 8. Free acceleration courses of the 3-phase of 315 kW, 6 kV induction motor controlled by MTC:
(a) stator current; (b) electromagnetic torque; (c) stator flux hodograph; (d) stator flux frequency; (e) slip of
the rotor; (f) rotational speed

beginning of the course results from the very small initial value of the Ψ_s flux. The following graphs show the results of computer simulations of the dynamics for the 315 kW, 3-phase motor, after the stepwise decrease of dc voltage supplying a converter from $U_{dc} = 8\,600$ V to half of its this value. From Fig. 9 it is clear that the magnetic field frequency as well as rotational speed act proportionally to match the voltage drop, whereas the flux is regulated within the required nominal band.

(a)

(b)

(c)

(d)

(e)
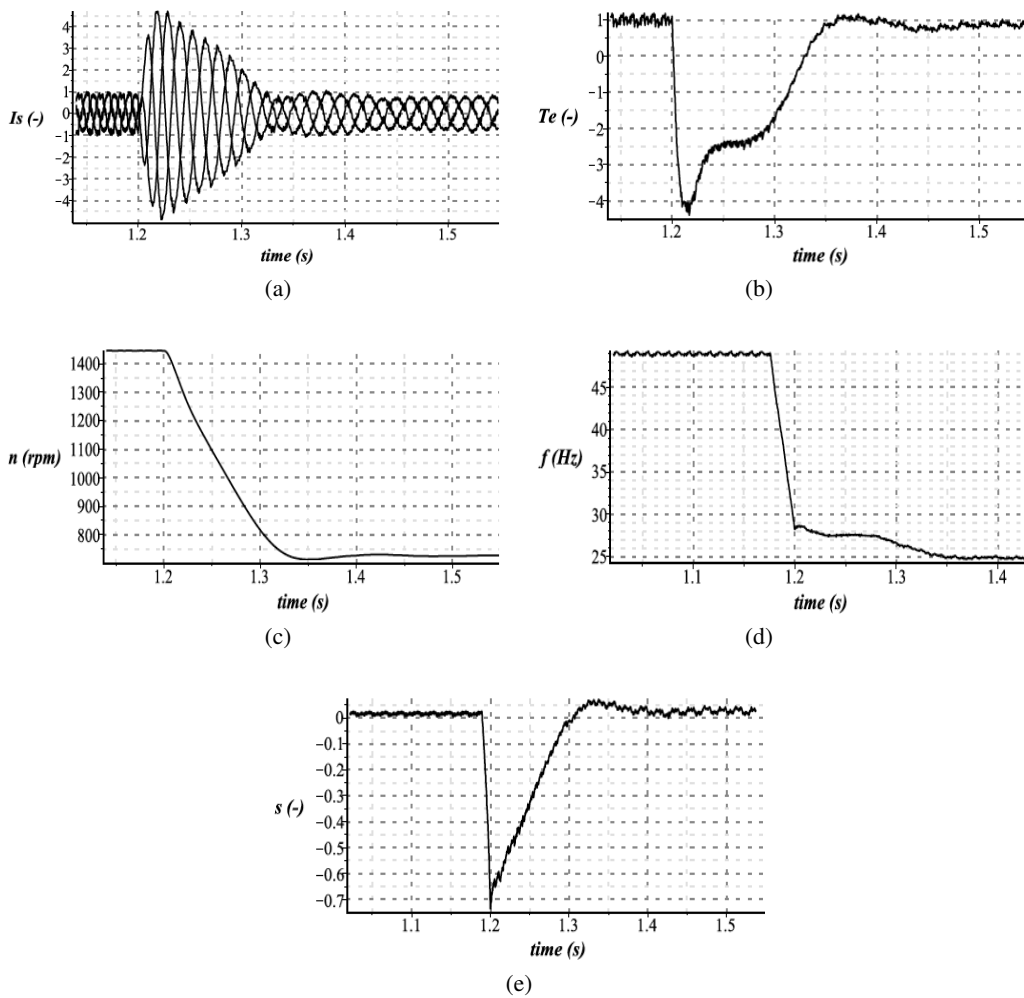
Fig. 9. Transients of the 315 kW, 6 kV induction motor controlled by MTC, after 50% step decrease of the dc voltage supplying the converter: (a) stator currents; (b) electromagnetic torque; (c) rotor speed; (d) magnetic field frequency f_s; (e) slip of the rotord

Fig. 10 shows the dynamic response of the 3-phase 315 kW induction motor drive to the linear field weakening from the nominal flux 19.5 Wb to 0.62 of this value.

(a)

(b)

(c)

(d)

(e)
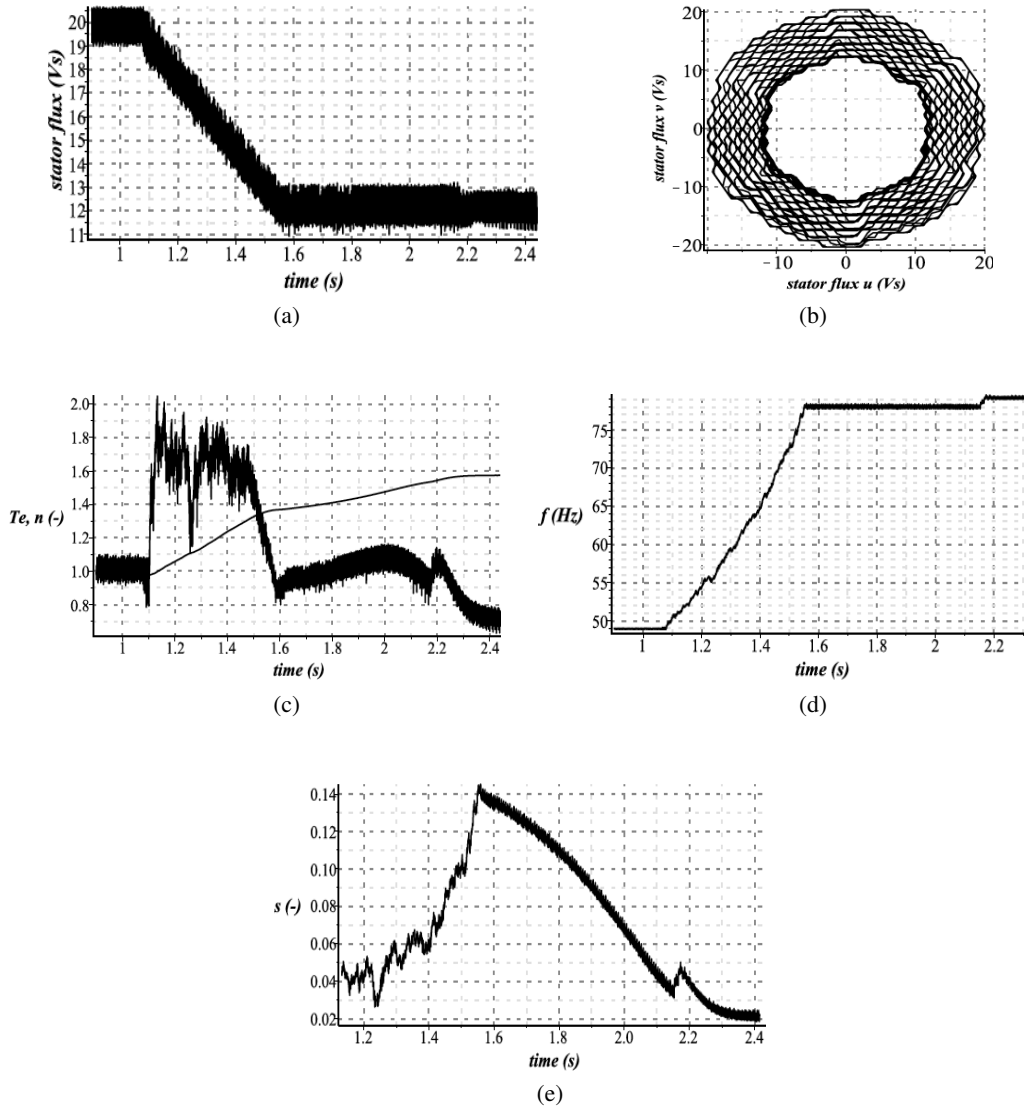
Fig. 10. Transients during magnetic field linear decrease for the 315 kW, 6 kV motor with MTC control:
(a) flux amplitude; (b) flux hodograph; (c) torque and rotor speed; (d) stator flux frequency; (e) slip

Fig. 11 presents the dynamic courses of the 315 kW motor drive during the linear decrease of the required speed and proportional decrease of the dc voltage supplying a converter. There is a comparison of results obtained without and with additional simple PI control of the speed, with respect to a given speed line. The results show that the MTC control of the drive by the dc supply level works effectively.
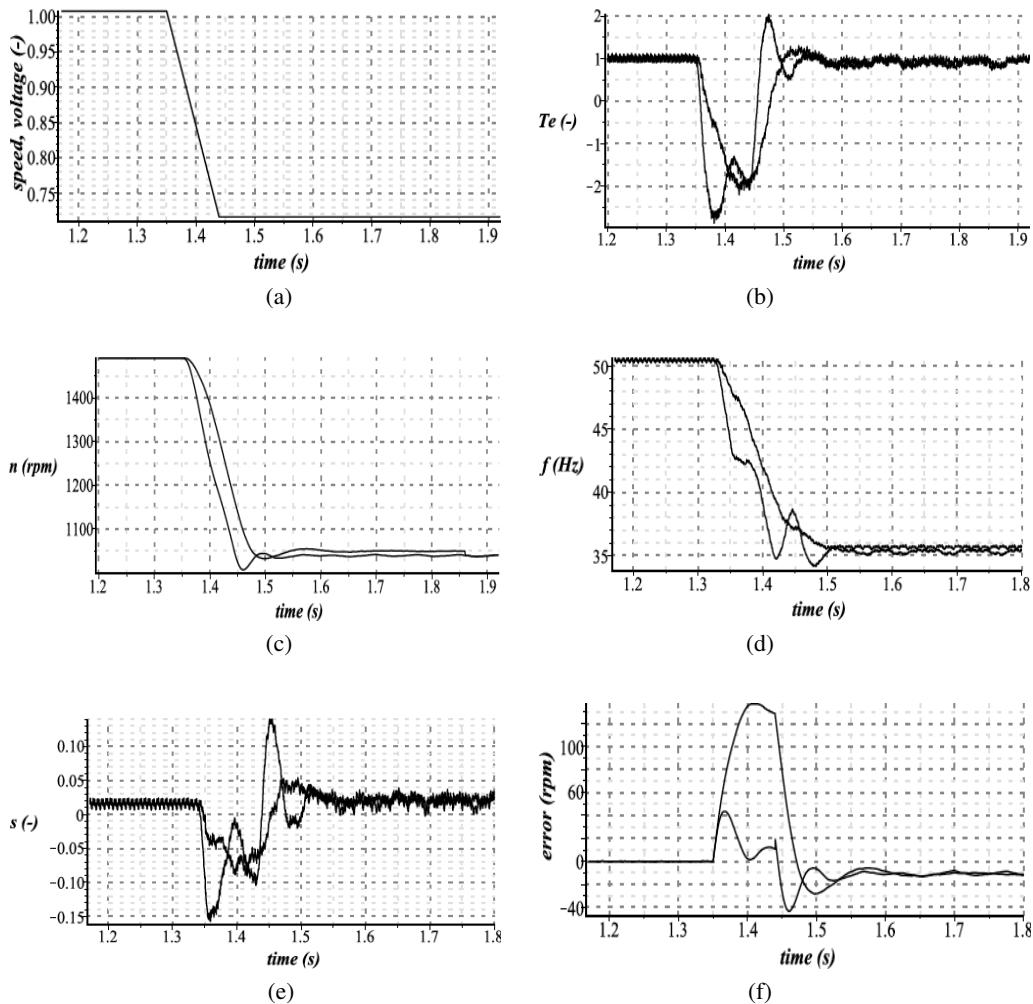
Fig. 11. Transients of the 315 kW, 6 kV induction motor drive, controlled by MTC, along given speed and voltage lines: (a) required speed and dc voltage lines; (b) electromagnetic torque; (c) rotor speed; (d) stator flux frequency; (e) slip of the rotor; (f) error of the regulation. In each figure there are compared courses: one with an additional PI regulation of the dc voltage and the second one without it

6. Conclusions

This paper presents a new effective method for induction motor drive control, called MTC, which forms a simplified derivative of the DTC considering control algorithm, but with the resulting characteristics similar to the ones for traditional dc motors. The application of this method offers good quality of dynamic courses and a simple control algorithm. The main control of the drive is based on the decrease of dc voltage supplying a converter for the speeds lower from the nominal or a decrease of the stator flux magnitude to increase the speed above the nominal value,

while a simplified DTC switching scheme is followed. Generally, this method of control results in transients and steady-state characteristics quite similar to the characteristics of separately excited dc commutator motors controlled by dc armature voltage or field weakening. The method is more effective in terms of reducing switching frequency in comparison to both FOC and DTC. The detailed characteristics of this control method depend on a way in which dc voltage is controlled, the sampling period, and the breadth of the band of flux magnitude stabilization. The variety of specific control methods that are used to control dc motor drives are directly applicable to MTC of induction drives via control of dc voltage supplying the converter.

References

[1] Casadei D., Serra G., Tani A., Zarri L., *Assessment of direct torque control for induction motor drives*, Bulletin of Polish Academy of Science: Technology, vol. 54, no. 3, pp. 237–254 (2006).

[2] Sorchini Z., Krein P.T., *Formal Derivation of Direct Torque Control for Induction Machines*, IEEE Transactions on Power Electronics, vol. 21, no. 5, pp. 1428–1436 (2006).

[3] Casadei D., Profumo F., Serra G., Tani A., *FOC and DTC: Two Viable Schemes for Induction Motor Torque Control*, IEEE Transactions on Power Electronics, vol. 17, no. 5, pp. 779–787 (2002).

[4] Kenny B.H., Lorentz R.D., *Stator-and-Rotor-Flux-Based Deadbeat Direct Torque Control of Induction Machines*, IEEE Transactions on Power Electronics, vol. 39, no. 4, pp. 1093–1101 (2003).

[5] Buja G.S., Kazmierkowski M.P., *Direct torque control of PWM inverter-fed AC motors – a survey*, IEEE Transactions on Industrial Electronics, vol. 51, no. 4, pp. 774–757 (2004).

[6] Khorammi F., Krishnamurthy P., Melkote H., *Modelling and Adaptive Nonlinear Control of Electric Motors*, Springer, Berlin, Heilderberg, New York (2003).

[7] Marino R., Tomei P., Verelli C.M., *Induction Motor Control Design*, Springer, London (2010).

[8] Wach P., *Induction Machine in Electric Drives*, in: *Dynamics and Control of Electrical Drives*, Springer, Berlin, Heilderberg, pp. 109–280 (2011).

[9] Hickiewicz J., Macek-Kamińska K., Wach P., *A simulation of common-bus drives in power plants*, Archive fur Elektrotechnik, vol. 75, pp. 293–302 (1992).

[10] Kim S.-H., Sul S.-K., *Maximum torque control of induction machine in the field weakening region*, IEEE Transactions on Industry Applications, vol. 31, no. 4, pp. 787–79 (1995).

[11] Garg R., Mahajan P., Gupta N., Saroa H., *A comparative study between field oriented control and direct torque control of AC traction motor* (2014), DOI: 10.1109/CRAIE.2014.6909201.

[12] Ambrozic V., Buja G.S., Menis R., *Band-constrained technique for direct torque control of induction motor*, IEEE Transactions on Industrial Electronics, vol. 51, no. 4, pp. 776–784 (2004).

[13] Ohuma T., Doki S., Okuma S., *Maximum torque control with inductance setting of extended EMF observer* (2009), DOI: 10.1109/EICON.2009.5414661.

[14] Krumov A.V., *Maximum torque high efficiency microprocessor based control of induction motors*, Proc of MIPRO 34-th Int Convention, pp. 800–804, inspec: 12137508 (2011).

[15] Boulghasoul Z., Elbacha A., Elwarraki E., Yousufi D., *Combined Vector and Direct Torque Control - an experimental review and evaluation* (2011), DOI: 10.1109/ICMCS.2011.5945662.

[16] Lai Y.-S., Chen J.-H., *A new approach to direct torque control of induction motor drives for constant inverter switching frequency and torque ripple reduction*, IEEE Transactions on Energy Conversion, vol. 16, no. 3, pp. 220–227 (2001).